An immune infiltration-related long non-coding RNAs signature predicts prognosis for hepatocellular carcinoma

Gen Li[1], Shaodian Xu[2], Shuai Yang[1], Cong Wu[1], Liangliang Zhang[1] and Hongbing Wang[1]*

[1]Beijing Hospital of Traditional Chinese Medicine, Capital Medical University, Beijing, China, [2]Xuanwu Hospital, Capital Medical University, Beijing, China

Background: With a high incidence and dismal survival rate, hepatocellular carcinoma (HCC) tops the list of the world's most frequent malignant tumors. Immunotherapy is a new approach to cancer treatment, and its effect on prolonging overall survival (OS) varies from patient to patient. For a more effective prognosis and treatment of HCC, we are committed to identifying immune infiltration-related long non-coding RNAs (IIRLs) with prognostic value in hepatocellular carcinoma.

Methods: In our study, we calculated immune scores of 369 hepatocellular carcinoma samples from the Cancer Genome Atlas (TCGA) database by using an estimation algorithm, and obtained long non-coding RNAs (lncRNAs) associated with immune infiltration by using Weighted Gene Co-expression Network analysis (WGCNA). For training cohort, univariate Cox, least absolute shrinkage and selection operator (Lasso) and multivariate Cox regression analysis were used to determine prognostic IIRLs, we established a prognostic IIRLs signature. By testing cohort and entire cohort, we confirmed that the signature is practical. The prognosis of people with different clinicopathological stages and risk scores were predicted by the nomogram we constructed. In addition, Immune cell infiltration analysis and prediction of therapeutic drugs were performed.

Results: 93 IIRLs were obtained by WGCNA. Furthermore, the prognostic value of these IIRLs were evaluated by using univariate Cox, Lasso and multivariate Cox analysis. Four IIRLs were used to create a signature with a prognosis. Time-related receiver operating characteristic (ROC) curve revealed that this model had an acceptable prognostic value for HCC patients. By using univariate and multivariate Cox regression analysis, this risk score has been shown to be an independent prognostic factor for HCC. The nomogram we made showed good predictions. Except for that, the treatment with immune checkpoint inhibitors (ICI) was likely to be more effective for low-risk patients.

Conclusion: Based on four IIRLs, a prognostic signature was created in this research showed good accuracy in predicting OS. This study also provided valuable references for Immunotherapy of hepatocellular carcinoma.

Introduction

As the seventh most common cancer worldwide, fatality rate of primary liver cancer is second among cancers (Bray et al., 2018; Chidambaranathan-Reghupaty et al., 2021). Hepatocellular carcinoma (HCC) is the most frequent kind of liver cancer, accounting for around 90% of primary liver cancer, and its incidence is on the rise worldwide (Kulik and El-Serag, 2019; Llovet et al., 2021a). However, the 5-years survival rate for HCC is very low (Jemal et al., 2017). In the treatment of hepatocellular carcinoma, HCC patients are staged according to the Barcelona Clinic Liver Cancer (BCLC) staging system (Llovet et al., 1999; European Association for the Study of the Liver, 2018; Llovet et al., 2021b). Resection, transplantation and local ablation are choices for patients with incipient hepatocellular carcinoma, while transcatheter arterial chemoembolization (TACE) is the first choice for patients at intermediate stage, and systemic therapy is preferred for people with advanced hepatocellular carcinoma (Llovet et al., 2021a). The extracellular matrix, blood vessels, immune cells, neurons, and other biological activities surrounding a tumor are known as the tumor microenvironment (TME), and they have strong ties to tumor development and response to therapy (Fridman et al., 2012; Kim et al., 2020). Immunotherapy has evolved over the past decade to become a new way to treat advanced tumors (Galon and Bruni, 2019; Cherkassky et al., 2022), and Immune checkpoint inhibitor (ICI) is a type of immunotherapy. As a second-line agent for systemic therapies, ICI is applied to HCC patients. If sorafenib failed, advanced HCC may be treated with either of three authorized regimens: regorafenib, cabozantinib, or ramucirumab. In addition, nivolumab (anti-PD1 inhibitors) and pembrolizumab (anti-PD1 inhibitor) are approved by the Food and Drug Administration (FDA) as single agents, and the combination including ipilimumab (CTLA4 monoclonal antibody) and nivolumab has been given the green light (Yau et al., 2020; Llovet et al., 2021a). With an objective response to ICI regimens, the average overall survival time for HCC patients is more than 30 months (Yau et al., 2020; Llovet et al., 2022). The result of the response to ICI monotherapy is used to enhance OS endpoints in clinical trials. There has been a long-term search for predictable clinical and tissue biomarkers, but some cannot be applied clinically due to their low sensitivity (Pinero et al., 2020; Llovet et al., 2022). It is urgent for us to find immune-related biomarkers that can forecast prognosis and therapy sensitivity in HCC.

The term "long non-coding RNA" (lncRNA) refers to non-coding RNAs that are longer than 200 nucleotides but playing no major role in protein coding (Wang et al., 2011). More and more evidences have shown that lncRNAs are essential components of the immune system and have the ability to control immune cell differentiation and function in cancer (Denaro et al., 2019; Wu et al., 2020). A study about HCC shows that the lnc-epidermal growth factor receptor (lnc-EGFR) encourages the development of Treg cells and prevents the activity of cytotoxic T lymphocytes (CTLs) (Jiang et al., 2017). Another hepatocellular carcinoma study shows that lncRNA nuclear enriched transcript 1 (NEAT1) inhibits the antitumor activity of CD8+T-cell and promotes their apoptosis through the Mir-155/TIM-3 pathway (Yan et al., 2019). Such being the case, Discovering lncRNAs associated to immune infiltration that is crucial for clinical prognosis and therapy.

In our study, we used the lncRNA dataset of HCC patients in the Cancer Genome Atlas (TCGA) to create a model of prognostic risk associated with immune infiltration. We elucidated its ability to predict overall survival of HCC patients. We also analyzed the correlation between the risk score constructed on the basis of immune infiltration-related lncRNAs (IIRLs) and immune cells and predicted the potential treatment drugs with different drug sensitivity between two groups.

Materials and methods

Data access to hepatocellular carcinoma

The RNA-sequencing (RNA-seq) transcriptomic data and clinicopathological characteristics of liver hepatocellular carcinoma (LIHC) were downloaded from The Cancer Genome Atlas (TCGA) database (https://portal.gdc.cancer.gov/). There were 374 tumor samples and 50 nearby tissues in the original data set. The sample data and clinical information were combined, excluding the adjacent tissue samples. The analytic data set for our research, consisting of 369 samples of hepatocellular carcinoma, was finally identified. According to the data, it was divided into mRNA data and lncRNA data.

Screening for immune infiltration-related lncRNAs

To determine the ImmuneScore for each HCC sample, we utilized the ESTIMATE package (Yoshihara et al., 2013) from the R suite. Through the lncRNA data, the WGCNA package (Langfelder and Horvath, 2008) in the R suite was used to create a scale-free co-expression network. The modules associated with the ImmuneScore were selected and the lncRNAs in the modules were extracted for subsequent analysis.

Construction of an immune infiltration-related lncRNAs prognostic signature

369 samples were used with 185 for training and 184 for testing. According to univariate Cox analysis, prognostic relevance of IIRLs was assessed in the training cohort. LncRNAs with $p < 0.05$ were considered to be promising candidates. Using the candidate lncRNAs and the glmnet package (Friedman et al., 2010), we constructed a LASSO regression model. Making use of the survival package, we obtained the hazard ratios (HR) and regression coefficients by introducing lncRNAs into a multivariate Cox model. We applied regression coefficients to construct a risk score. The following procedure was used to calculate the risk score

$$\text{Risk score} = \sum_{i=1}^{n} Coefi^{*}Expi$$

The expression of IIRLs in the signature was represented by Expi, with Coefi representing the regression coefficients. According to the median risk score, the patients were sorted into high-risk and low-risk groups. We examined the performance of prognostic indicators in terms of overall survival (OS) by using Kaplan Meier (KM) survival and receiver operating characteristic (ROC) curve analysis. Validation of the prognostic signature developed by training cohort was performed on testing cohort and entire cohort.

Evaluation of prognostic factors and development of a predictive nomogram

KM survival analysis was carried out in two groups to clarify differences among subgroups based on gender, age, grade, and American Joint Committee on Cancer (AJCC) stages. Clinical features and risk score were applied to univariate and multivariate Cox regression analyses in order to determine whether they were independent prognostic factors. The line chart was applied to predict 1-year, 3-years, and 5-years survival rates. We used concordance index (C-index) and calibration curves to assess the stability of this model.

Functional enrichment analysis

According to the limma package (Ritchie et al., 2015), different analysis was conducted on mRNA data to clarify the biological function differences between two groups. We used the gene set enrichment analysis (GSEA) function in clusterProfiler (Yu et al., 2012; Wu et al., 2021a) to perform Gene Ontology (GO) and Kyoto Encyclopedia of Genes and Genomes (KEGG) enrichment analysis for difference analysis results.

Immune correlation analysis

The single-sample gene set enrichment analysis (ssGSEA) algorithm was used to assess immune-related function of each sample (Hanzelmann et al., 2013). We obtained the infiltration results of 22 immune cell subtypes in each sample by using CIBERSORT algorithm (Newman et al., 2015) from the TIMER (Li et al., 2016; Li et al., 2017; Li et al., 2020) database. We examined the variations in immune cells in two groups as well as the relationships among various immune cells. We obtained the immune cell infiltration results of different algorithms from the TIMER (29–31) database, and found out the relationship between risk scores and different immune cells.

Evaluation of the Model's importance in predicting drug susceptibility

The Wilcoxon signed-rank test was used to compare immune checkpoint gene expression levels between two groups for PD-1, PDL-1, CTLA-4, LAG-3, and VSIR. From the Cancer Immunome Atlas (TCIA) database (https://tcia.at/), we retrieved the Immunophenoscores (IPS) of HCC patients. We compared the IPS between two groups in various immunotherapy choices in order to predict the sensitivity of immunotherapy. Using the pRRophetic package, we tallied the half-maximal inhibitory concentration (IC50) of standard chemotherapy and molecular targeted medicines for each sample to assess the signature's utility in predicting the success of HCC treatment (Geeleher et al., 2014a; Geeleher et al., 2014b). Wilcoxon signed-rank test ($p < 0.001$ as significant level) was used to compare the IC50 between two groups. We used the spearman rank correlation to determine whether there was a connection between risk scores and IC50 (with a cutoff of $p < 0.001$ and an absolute value of the Spearman rank correlation coefficient $|R| \geq 0.25$).

Results

Identify immune infiltration-related lncRNAs

The flow chart of study was shown in Figure 1. 369 LICH sample data were filtered out of low-expression RNA-seq data and converted into mRNA data and lncRNA data according to the data. We used WGCNA to analyze lncRNA data. We selected a soft threshold of 3 (Figures 2A,B) and chose 30 as the minimum number of lncRNAs in the module. We set the threshold to 0.25 of cutting height to combine any potentially similar modules, resulting in 16 modules (Figure 2D). The salmon module was highly positively correlated with ImmuneScore (correlation coefficient R = 0.78, $p < 0.001$) (Figure 2C). Thus, we obtained 93 IIRLs.
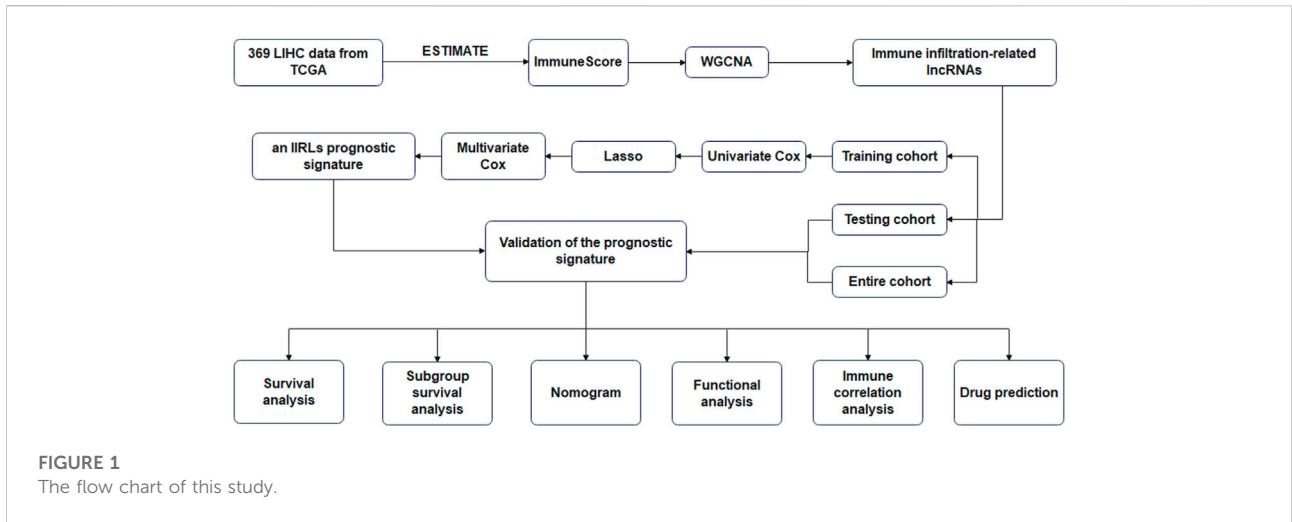
FIGURE 1
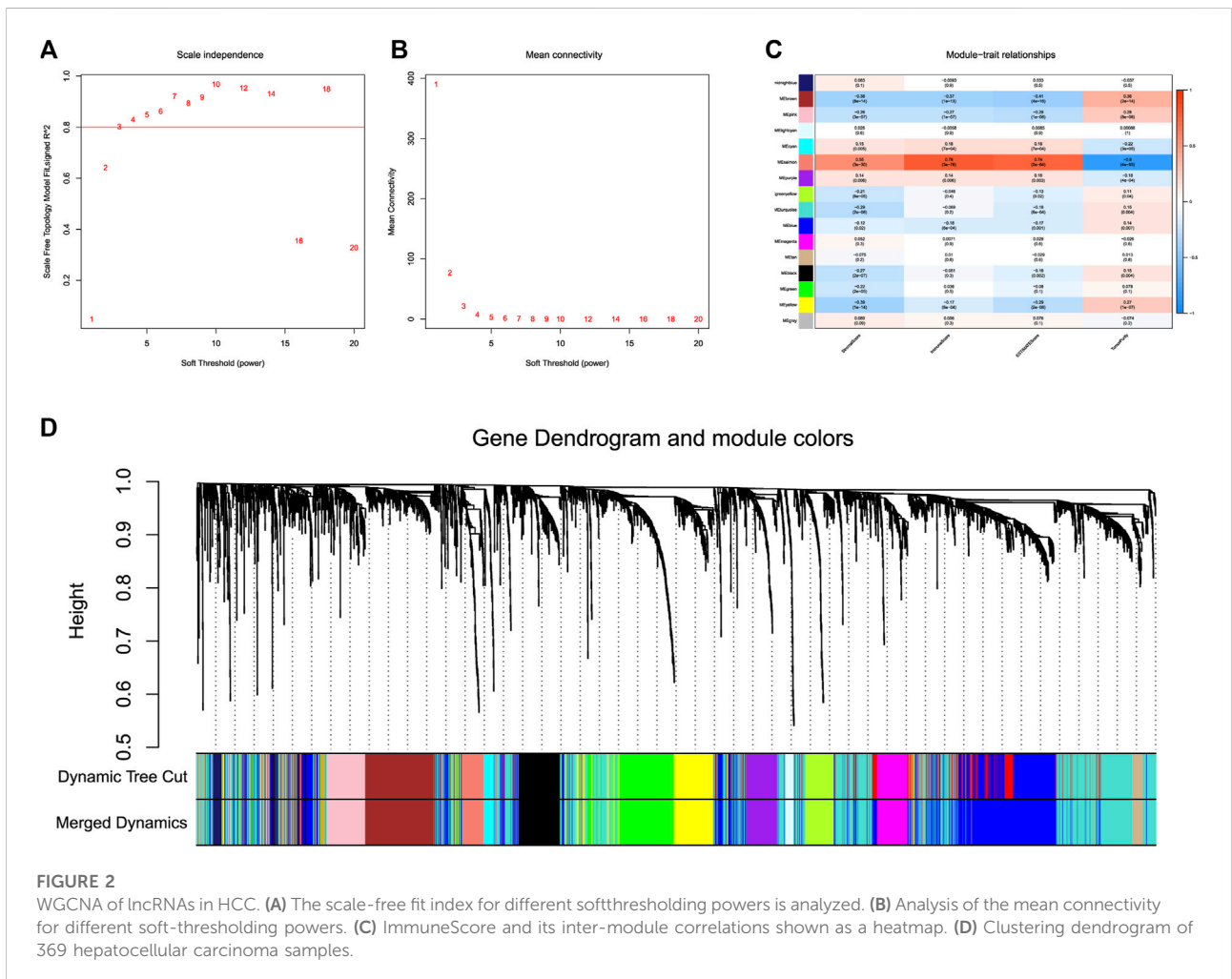The flow chart of this study.

FIGURE 2
WGCNA of lncRNAs in HCC. **(A)** The scale-free fit index for different softthresholding powers is analyzed. **(B)** Analysis of the mean connectivity for different soft-thresholding powers. **(C)** ImmuneScore and its inter-module correlations shown as a heatmap. **(D)** Clustering dendrogram of 369 hepatocellular carcinoma samples.

TABLE 1 The baseline data of three cohorts.

	Total (*n* = 369)	Test (*n* = 184)	Train (*n* = 185)	p-value
Age				
≤65	232 (62.87%)	124 (67.39%)	108 (58.38%)	0.0791
>65	136 (36.86%)	59 (32.07%)	77 (41.62%)	
Unknow	1 (0.27%)	1 (0.54%)	0 (0%)	
Gender				
Female	120 (32.52%)	68 (36.96%)	52 (28.11%)	0.0886
Male	249 (67.48%)	116 (63.04%)	133 (71.89%)	
Grade				
G1	55 (14.91%)	28 (15.22%)	27 (14.59%)	0.3318
G2	177 (47.97%)	86 (46.74%)	91 (49.19%)	
G3	120 (32.52%)	63 (34.24%)	57 (30.81%)	
G4	12 (3.25%)	3 (1.63%)	9 (4.86%)	
Unknow	5 (1.36%)	4 (2.17%)	1 (0.54%)	
Stage				
Stage I	171 (46.34%)	86 (46.74%)	85 (45.95%)	0.9712
Stage II	86 (23.31%)	44 (23.91%)	42 (22.7%)	
Stage III	83 (22.49%)	42 (22.83%)	41 (22.16%)	
Stage IV	5 (1.36%)	2 (1.09%)	3 (1.62%)	
Unknow	24 (6.5%)	10 (5.43%)	14 (7.57%)	
T				
T1	181 (49.05%)	93 (50.54%)	88 (47.57%)	0.8125
T2	94 (25.47%)	45 (24.46%)	49 (26.49%)	
T3	77 (20.87%)	35 (19.02%)	42 (22.7%)	
T4	13 (3.52%)	7 (3.8%)	6 (3.24%)	
Unknow	4 (1.08%)	4 (2.17%)	0 (0%)	
M				
M0	265 (71.82%)	132 (71.74%)	133 (71.89%)	0.6303
M1	4 (1.08%)	1 (0.54%)	3 (1.62%)	
Unknow	100 (27.1%)	51 (27.72%)	49 (26.49%)	
N				
N0	250 (67.75%)	121 (65.76%)	129 (69.73%)	0.1226
N1	4 (1.08%)	4 (2.17%)	0 (0%)	
Unknow	115 (31.17%)	59 (32.07%)	56 (30.27%)	

Construction of an immune infiltration-related lncRNAs prognostic signature

Dividing the dataset into training and testing cohorts in a random fashion, we compared the baseline data of three cohorts (Table 1). The univariate Cox regression performed on training cohort revealed that eight IIRLs were relevant with HCC prognosis (Figure 3A). These genes were then subjected to LASSO regression, and seven IIRLs were discovered following LASSO regression (Figures 3B,C). We found out four IIRLs (LINC01871, AC011407.1, LINC01094, AC006369.1) by using multivariate Cox regression. LINC01871, AC011407.1, and AC006369.1 were protective factors for HCC, while

LINC01094 was a risk factor for HCC (Figures 3D–G). The following risk score formula was used to produce an IIRLs prognostic signature (Table 2).

Risk score = (1.2429*Exp LINC01094) -(0.3043*Exp LINC01871) -(2.199*Exp AC011407.1) -(1.8701*Exp AC006369.1).

Assessment of an immune infiltration-related lncRNAs prognostic signature

Each sample in the training cohort had its risk score determined by the risk score methodology. According to
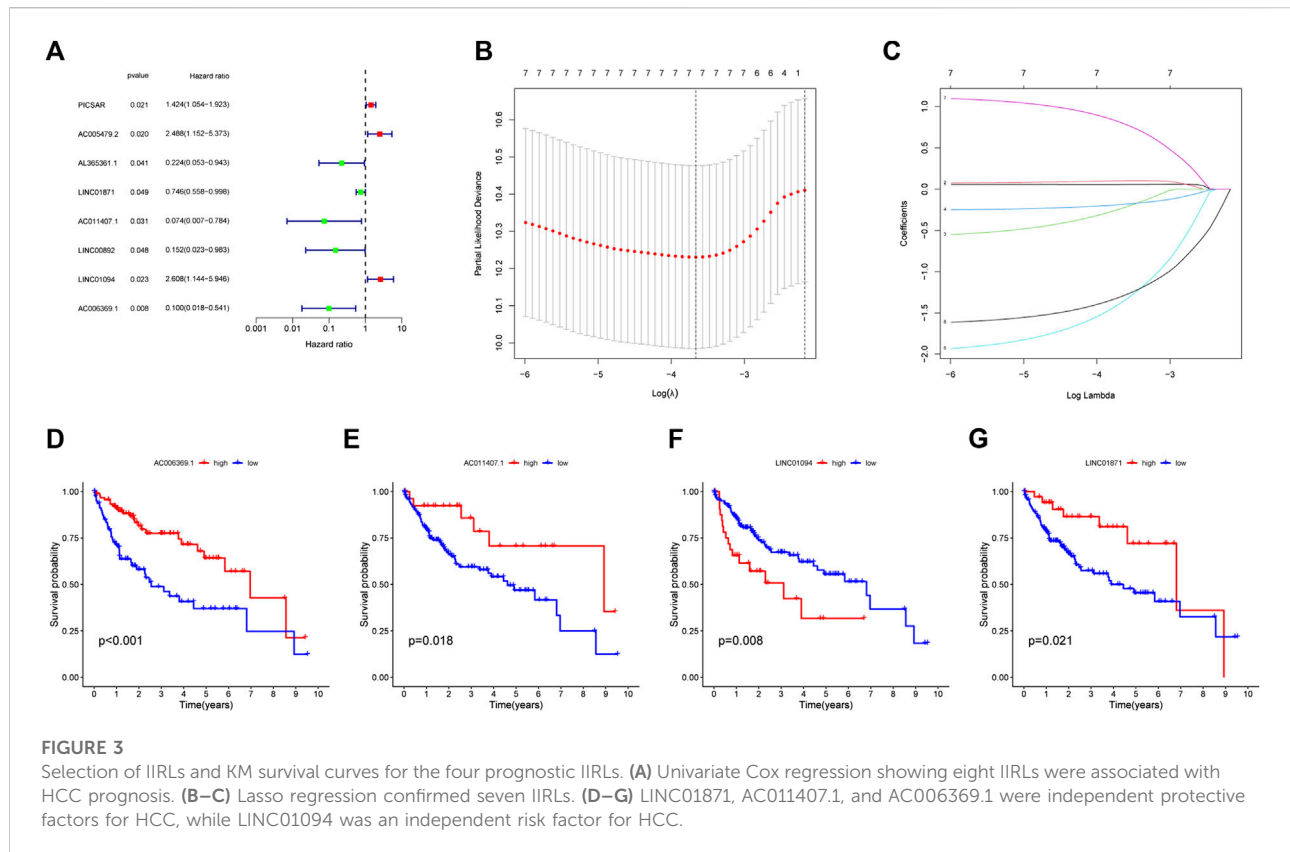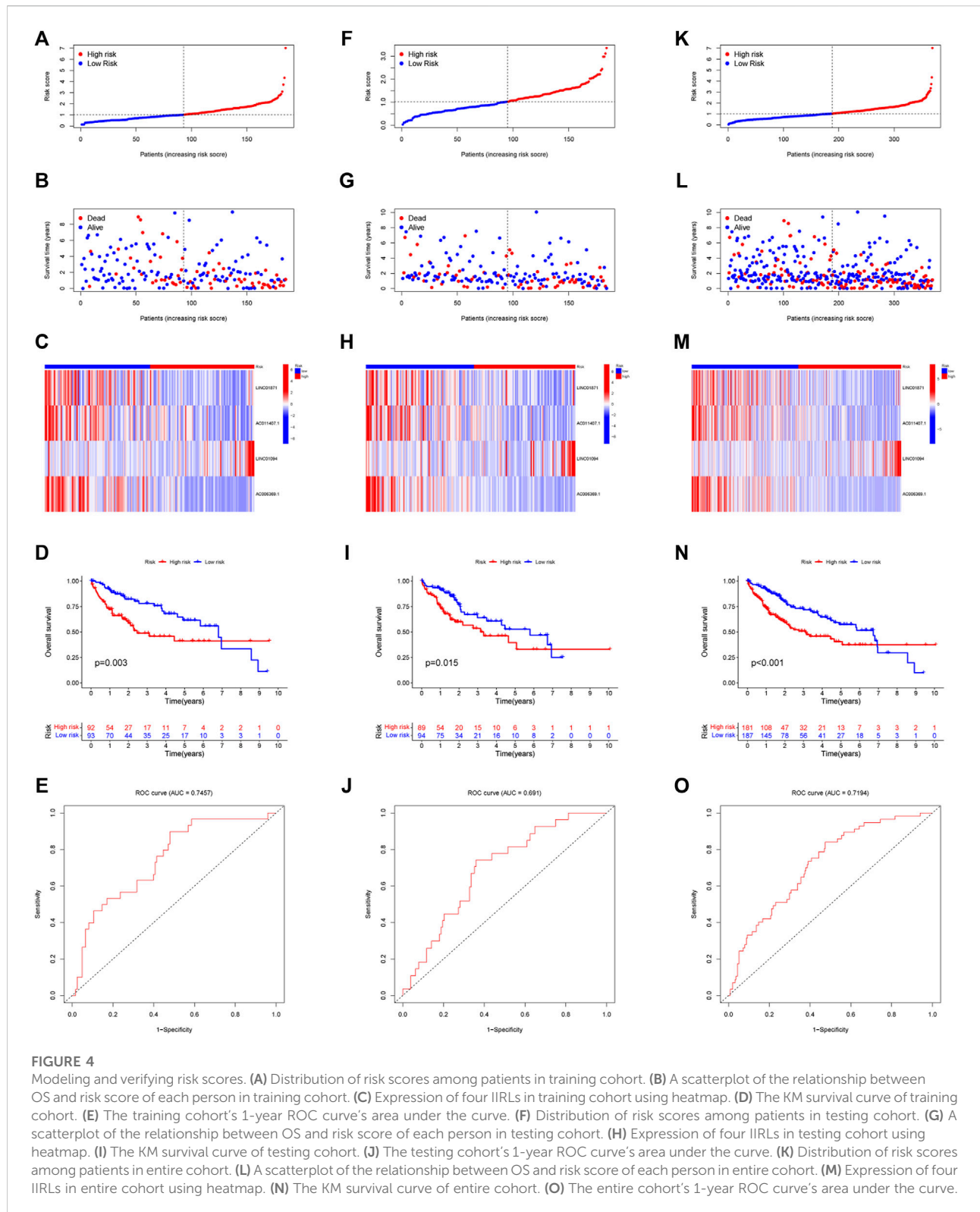
FIGURE 3
Selection of IIRLs and KM survival curves for the four prognostic IIRLs. **(A)** Univariate Cox regression showing eight IIRLs were associated with HCC prognosis. **(B−C)** Lasso regression confirmed seven IIRLs. **(D−G)** LINC01871, AC011407.1, and AC006369.1 were independent protective factors for HCC, while LINC01094 was an independent risk factor for HCC.

TABLE 2 Multivariate Cox results for IIRLs.

Id	Coef	HR	HR.95 L	HR.95 H	*p*-value	Risk
LINC01871	−0.3043	0.7377	0.543	1.0021	0.0516	Low
AC011407.1	−2.199	0.1109	0.0088	1.3988	0.089	Low
LINC01094	1.2429	3.4658	1.551	7.7444	0.0024	High
AC006369.1	−1.8701	0.1541	0.029	0.8186	0.0282	Low

the median risk score (1.025), we classfied all patients into low-risk and high-risk (Figure 4A). A progressive decline in survival time and an increase in mortality were seen in conjunction with an increase in risk score (Figure 4B). Heatmaps were used to display the expression levels of four IIRLs (LINC01871, AC011407.1, LINC01094, and AC006369.1) in the training cohort (Figure 4C). The finding shows two groups had significantly different OS, according to the KM survival curve (*p* = 0.003) (Figure 4D). By time-dependent ROC curve, we predicted lncRNA biomarkers with an AUC of 0.7457 (Figure 4E). The signature was then tested on testing cohort and entire cohort to ensure its accuracy (Figures 4F–O). Throughout testing cohort and entire cohort, we found the high-risk group had a substantially shorter OS compared to the low-risk

group. Moreover, the AUCs for testing cohort and entire cohort were 0.691 and 0.7194, which indicated that this prognostic signature has good stability.

Clinical value of the prognostic signature

Figure 5A showed the heatmap of clinical information of patients in two groups and we compared the two groups to see whether there were differences in clinical information. The distributions of AJCC stage and T-stage were different for the high-risk and low-risk groups (Figures 5B,C). Except for three subgroups (subgroup of female, subgroup of G3 and G4, subgroup of stage III and stage IV), OS was shorter for patients in the high-risk group (Figures 5D–K). For HCC

FIGURE 4
Modeling and verifying risk scores. **(A)** Distribution of risk scores among patients in training cohort. **(B)** A scatterplot of the relationship between OS and risk score of each person in training cohort. **(C)** Expression of four IIRLs in training cohort using heatmap. **(D)** The KM survival curve of training cohort. **(E)** The training cohort's 1-year ROC curve's area under the curve. **(F)** Distribution of risk scores among patients in testing cohort. **(G)** A scatterplot of the relationship between OS and risk score of each person in testing cohort. **(H)** Expression of four IIRLs in testing cohort using heatmap. **(I)** The KM survival curve of testing cohort. **(J)** The testing cohort's 1-year ROC curve's area under the curve. **(K)** Distribution of risk scores among patients in entire cohort. **(L)** A scatterplot of the relationship between OS and risk score of each person in entire cohort. **(M)** Expression of four IIRLs in entire cohort using heatmap. **(N)** The KM survival curve of entire cohort. **(O)** The entire cohort's 1-year ROC curve's area under the curve.

patients, we can see that the risk score was a significant risk factor connected to their prognosis by univariate Cox regression analysis (95% confidence interval (CI):

1.330–1.855, $p < 0.001$). In addition, AJCC stage (95%CI: 1.360–2.061, $p < 0.001$) was also closely related to prognosis (Figure 6A). Risk score remained a significant factor in

FIGURE 5
Comparison of overall survival (OS) between subgroups of individuals with different clinicopathological features. **(A)** The risk–clinical characteristic heatmap was used to visualize this relationship ($*p < 0.05$, $**p < 0.01$, and $***p < 0.001$). **(B)** Distribution of AJCC stage in two groups. **(C)** Distribution of T-stage in two groups. **(D–E)** Subgroup of gender (male and female). **(F–G)** Subgroup of age (≤65 years and >65 years). **(H–I)** Subgroup of grade (G1, G2, G3, and G4). **(J–K)** Subgroup of AJCC stage (I, II III, and IV).

multivariate Cox regression (HR = 1.384, 95% CI: 1.150–1.666, $p < 0.001$, Figure 6B). By ROC analysis, we confirmed that the risk score had higher accuracy in predicting patients compared with other clinicopathological features (Figure 6C). Comparative ROC curves for risk scores at one, three, and 5 years were created (Figure 6D). The 1-year risk score had the best predictive accuracy.

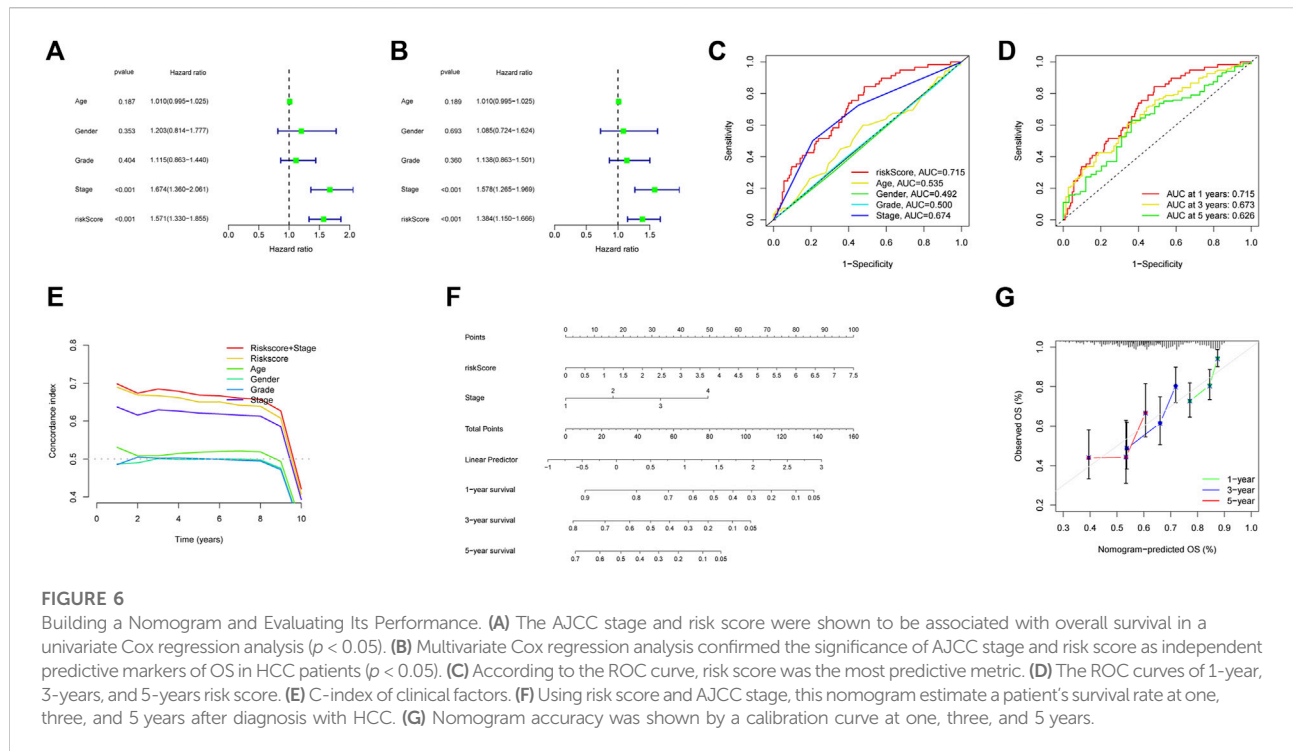## Building a nomogram and evaluating its performance

Based on risk score and AJCC stage, we made a nomogram by using multivariate Cox regression. When the index values for each AJCC stage and risk factor were added together, a prediction of survival at 1, 3, and 5 years could be made (Figure 6F). The concordance index shows strong stability in the nomogram (Figure 6E). The calibration curve also demonstrated that the anticipated survival lengths at 1, 3, and 5 years were consistent with the reference line (Figure 6G).

Functional enrichment analysis

We used the GSEA function to perform GO and KEGG enrichment analysis. GO analysis showed that they were significantly enriched in B cell mediated immunity, complement activation, humoral immune response mediated by circulating immunoglobulin, lymphocyte mediated immunity, immunoglobulin complex, T-cell receptor complex, and antigen binding (Figure 7A). According to KEGG analysis, they were significantly enriched in the following pathways: chemokine signaling pathway; complement and coagulation cascades; graft *versus* host disease; intestinal immune network for IgA production; natural killer cell mediated cytotoxicity; primary immunodeficiency; viral myocarditis (Figure 7B).

Immune correlation analysis

The ssGSEA immune function scores were performed based on each sample. With the exception of MHC class I, low-risk group had better immune function ratings than high-risk group ($p < 0.05$)

FIGURE 6
Building a Nomogram and Evaluating Its Performance. **(A)** The AJCC stage and risk score were shown to be associated with overall survival in a univariate Cox regression analysis ($p < 0.05$). **(B)** Multivariate Cox regression analysis confirmed the significance of AJCC stage and risk score as independent predictive markers of OS in HCC patients ($p < 0.05$). **(C)** According to the ROC curve, risk score was the most predictive metric. **(D)** The ROC curves of 1-year, 3-years, and 5-years risk score. **(E)** C-index of clinical factors. **(F)** Using risk score and AJCC stage, this nomogram estimate a patient's survival rate at one, three, and 5 years after diagnosis with HCC. **(G)** Nomogram accuracy was shown by a calibration curve at one, three, and 5 years.

([Figure 7C](#)). The number of individuals in low-risk group had a high ImmuneScore than in high-risk group. ([Figure 8A](#)). Using the CIBERSORT algorithm, we were able to determine the percentage of 22 different types of immune cells present in HCC patients. The boxplot clearly displayed the dissimilar distributions of immune cells between two groups. There were less CD8+ T-cell, resting memory CD4+ T-cell, Gamma delta T-cell, activated NK cells, and classically activated macrophages in high-risk group compared to low-risk group ([Figure 8B](#)). [Figure 8C](#) showed the correlation between various immune cells. [Figures 8D,E](#) demonstrated the distribution of 22 immune cells in two groups. When we examined the correlation between immune cells and risk score using various algorithms, the findings revealed that the majority of immune cells had a poor relationship with risk score ([Figure 8F](#)).
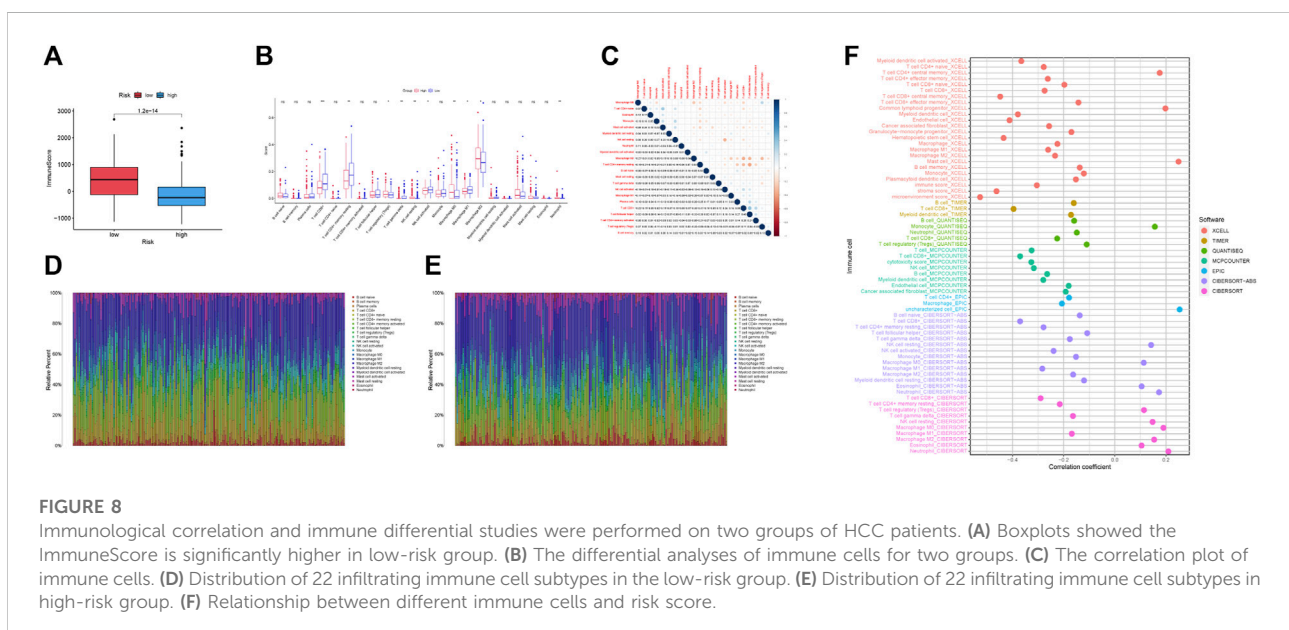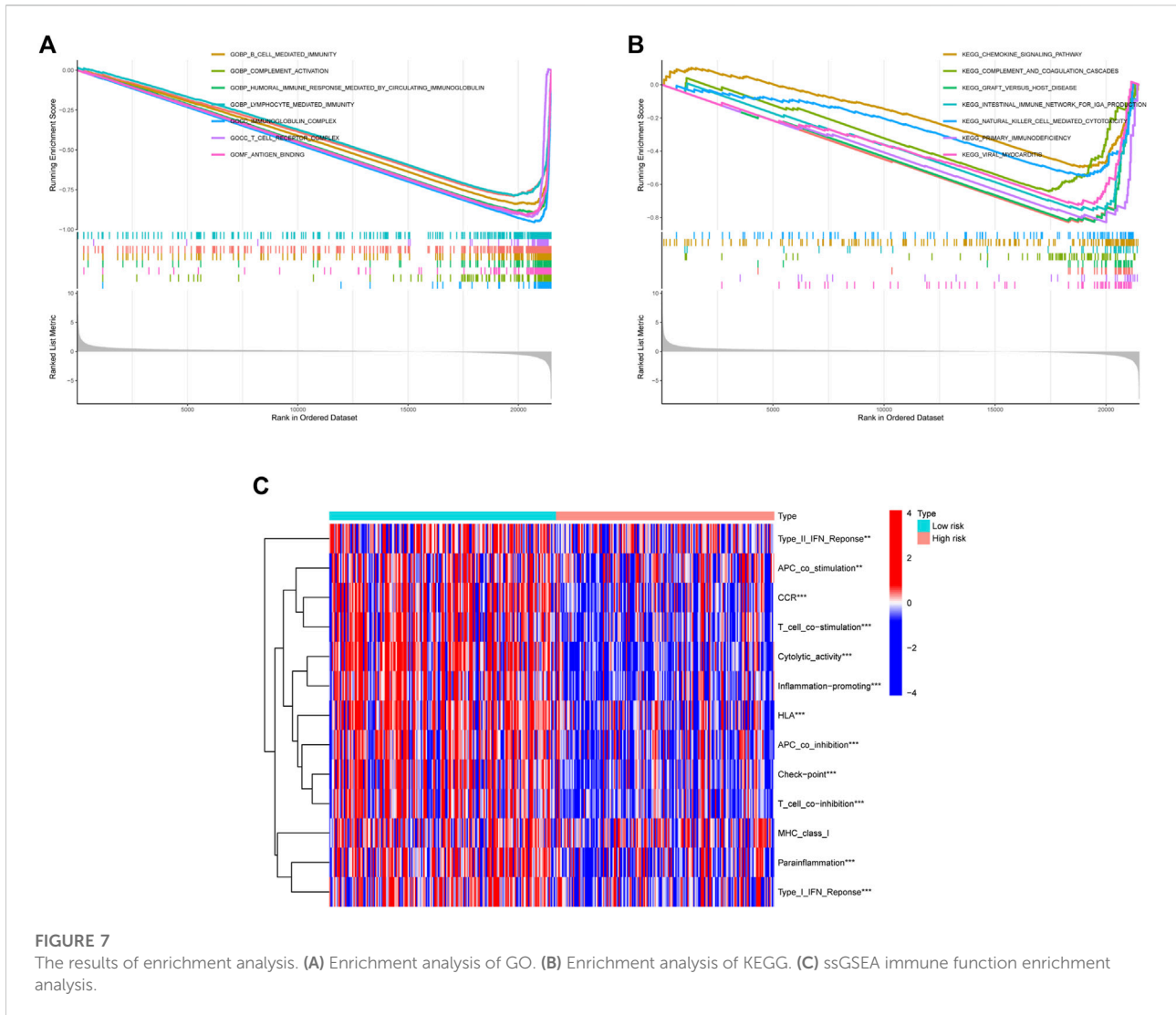
Drug prediction

The low-risk group had significantly greater expression levels of immune checkpoint genes ([Figure 9A](#)). The association of IPS with high-risk and low-risk groups was investigated. We used IPS, IPS-PD1, IPS-CTLA4, and IPS- PD1 + CTLA4 to evaluate the potential of risk scores application. The IPS, IPS-PD1, IPS-CTLA4, and IPS-PD1 + CTLA4 were different in two groups ($p < 0.05$) ([Figures 9B–E](#)). Based on the CGP database, drug IC50 information was obtained to predict treatment response, and epothilone. B may be a potential therapeutic drug for patients in high-risk groups ([Figures 9F, M](#)). Six drugs (temsirolimus, KU.55933, elesclomol, EHT. 1864,
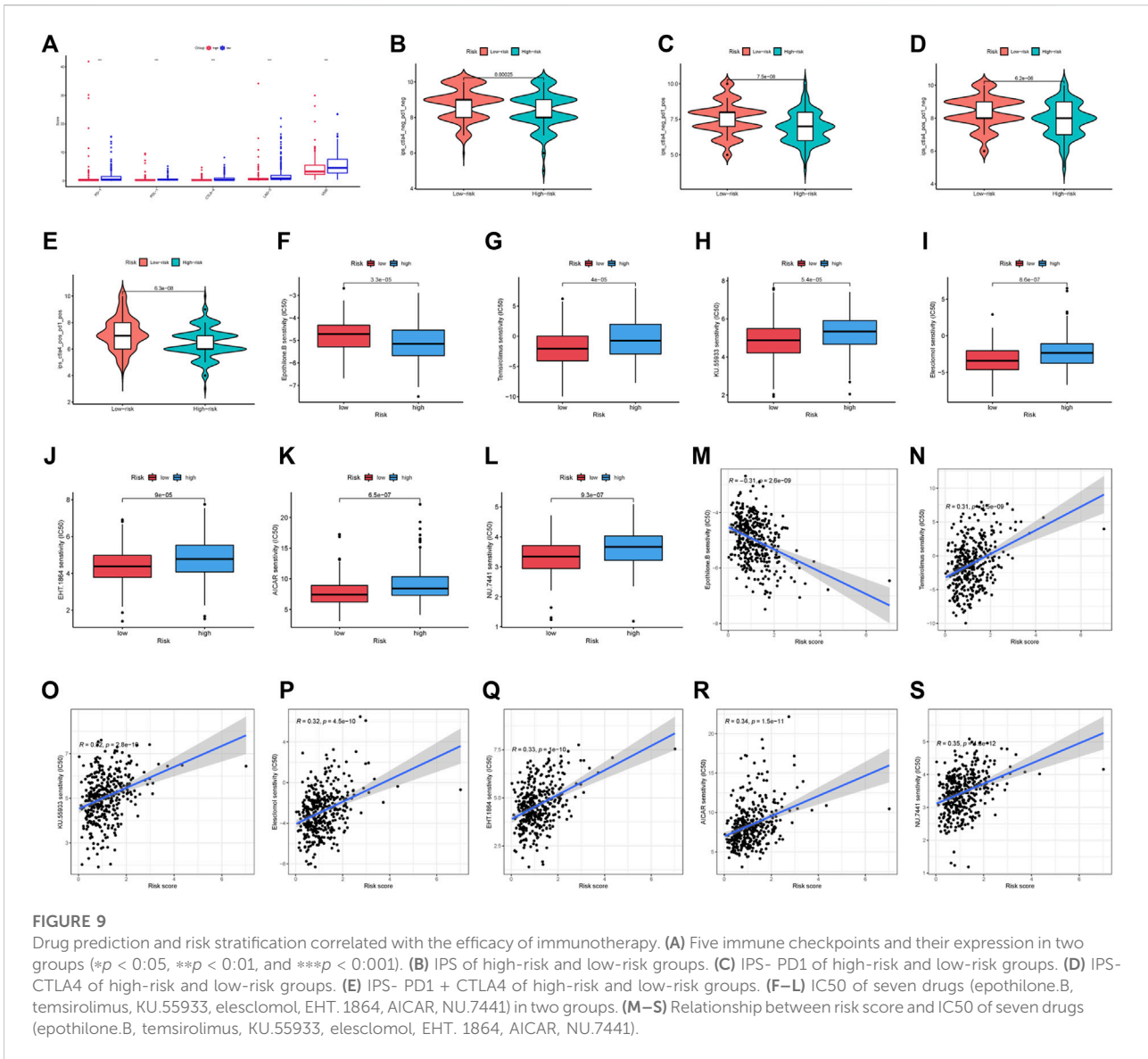
AICAR, NU.7441) were screened as potential therapeutic drugs for patients in low-risk group ([Figures 9G–L, N–S](#)).

Discussion

With the deepening of research on hepatocellular carcinoma and the improvement of therapeutic methods, the 5-years survival rate of patients is still low. TME is linked to tumor development and response to treatment, and immunotherapy is evolving into a novel approach to treating high-grade cancers. At present, a variety of ICIs have been applied to the second-line treatment of HCC systemic therapy, but they are only effective in hepatocellular carcinoma patients with immune response. For that reason, how to predict outcomes for people with HCC and guide the signature of immunotherapy has become increasingly crucial. LncRNAs are key players in the tumor immune system and can be used as potential prognostic biomarkers. In our study, we applied a combination of univariate Cox, LASSO, and multivariate Cox regression to establish an immune infiltration-related lncRNAs prognostic signature. The prediction performance of this signature was high. Patients classified as low risk have a longer expected survival time than those of high risk. Our final tally of four IIRLs suggests they may serve as both prognostic indicators and therapeutic targets for hepatocellular carcinoma.

Among the four IIRLs risk model, the biological mechanisms of LINC01871, AC011407.1, and AC006369.1 have not been reported to date. Based on bioinformatics analysis, some prognostic models constructed suggested that LINC01871 was related to immune

FIGURE 7
The results of enrichment analysis. **(A)** Enrichment analysis of GO. **(B)** Enrichment analysis of KEGG. **(C)** ssGSEA immune function enrichment analysis.

FIGURE 8
Immunological correlation and immune differential studies were performed on two groups of HCC patients. **(A)** Boxplots showed the ImmuneScore is significantly higher in low-risk group. **(B)** The differential analyses of immune cells for two groups. **(C)** The correlation plot of immune cells. **(D)** Distribution of 22 infiltrating immune cell subtypes in the low-risk group. **(E)** Distribution of 22 infiltrating immune cell subtypes in high-risk group. **(F)** Relationship between different immune cells and risk score.

FIGURE 9
Drug prediction and risk stratification correlated with the efficacy of immunotherapy. **(A)** Five immune checkpoints and their expression in two groups (∗*p* < 0:05, ∗∗*p* < 0:01, and ∗∗∗*p* < 0:001). **(B)** IPS of high-risk and low-risk groups. **(C)** IPS- PD1 of high-risk and low-risk groups. **(D)** IPS-CTLA4 of high-risk and low-risk groups. **(E)** IPS- PD1 + CTLA4 of high-risk and low-risk groups. **(F–L)** IC50 of seven drugs (epothilone.B, temsirolimus, KU.55933, elesclomol, EHT. 1864, AICAR, NU.7441) in two groups. **(M–S)** Relationship between risk score and IC50 of seven drugs (epothilone.B, temsirolimus, KU.55933, elesclomol, EHT. 1864, AICAR, NU.7441).

response (Chen et al., 2020; Ma et al., 2020; Mathias et al., 2021; Wang et al., 2021). To exert their functions, lncRNAs are used as signals, decoys, scaffolds, guides, or enhencers (Wang and Chang, 2011; El Khodiry et al., 2018). Therefore, the roles of these three lncRNAs in hepatocellular carcinoma should be further studied in the near future. Several studies have indicated that LINC01094 can act as an effective miR-577 sponge to promote the proliferation, invasion and metastasis of various tumors (Xu et al., 2020a; Dong et al., 2020; Luo et al., 2021). Targeting the miR-577/CHEK2/FOXM1 axis, LINC01094 promotes radioresistance in clear cell renal cell carcinoma (ccRCC) (Jiang et al., 2020). Apart from acting as an effective miR-577 sponge, LINC01094 can competitively bind to a variety of microRNAs to promote tumor progression (Xu et al., 2020b; Li and Yu, 2020; Zhu et al., 2020; Wu et al., 2021b; Chen et al., 2021; Liu et al., 2022). From our study, the expression of LINC01094 is clearly elevated in high-risk

group compared to low-risk group, which may promote the progress of HCC. Although LINC01094 is related to the progression of ccRCC, glioblastoma, and ovarian cancer (Xu et al., 2020b; Li and Yu, 2020; Chen et al., 2021), still no studies have shown a relationship between LINC01094 and the progression of HCC. Additional trials are needed to confirm whether or not LINC01094 may accelerate HCC development. The biological roles of lncRNAs in HCC including cell proliferation, cell death, metabolic reprogramming, angiogenesis, metastasis, inflammation and tumour immunity (Yu et al., 2018; Xie et al., 2021). The roles of lncRNAs in tumor immunity can be classified into the following five points (Yu et al., 2018): (Bray et al., 2018) bidirectional regulation of antigen release (Chidambaranathan-Reghupaty et al., 2021); participating in antigen presentation (Kulik and El-Serag, 2019); regulating immune cell differentiation during immune priming and activation

(Llovet et al., 2021a); influencing immune cells migration and T-cell infiltration (Jemal et al., 2017); affecting the recognition and killing of cancer cells. At present, there are no relevant studies on tumor immunity of these four IIRLs in HCC. For this reason, we think that these IIRLs can be deeply studied from five aspects of tumor immunity above.

GSEA enrichment results were mainly in immune related pathways. Compared to low-risk group, the expression of these pathways was considerably lower in high-risk group, according to the negative enrichment score. The results of immune function enrichment also demonstrated that the immune function of high-risk group decreased accordingly. Myeloid-derived suppressor cells (MDSCs), tumor-associated macrophages (TAMs), tumor associated neutrophils (TANs), regulatory T-cell (Treg) can achieve immune escape through immune suppression, thus promoting tumor development (Fu et al., 2019; Lawal et al., 2021). MDSCs can achieve immunosuppression by producing immunosuppressive factors (such as arginase, inducible nitric oxide synthase, IL-10, TGF-β) to inhibit cytotoxic T-cell and NK cell function (Gabrilovich and Nagaraj, 2009; Masucci et al., 2019; Lawal et al., 2021). There are two distinct phenotypes among TAMs, M1, and M2. The M2 phenotype promotes tumor initiation, progression, and metastasis *via* many pathways (Qian and Pollard, 2010; Yao et al., 2018). By activating the TLR4/TRIF/NF-B signaling pathway, HCC cells encourage the immunological evasion of HCC by boosting IL-1 secretion of TAMs (Zhang et al., 2018). According to their polarizing effects, Tans can be classified as either anti-tumor (N1) or pro-tumor (N2) phenotypes, and the degree of invasion of Tans is strongly correlated with tumor growth (Nicolas-Avila et al., 2017; Fu et al., 2019). Inducing apoptosis in CD8$^+$ T lymphocytes through nitric oxide generation mediated by tumor necrosis factor alpha (TNF-α) is how TANs accomplish their immunosuppressive effects (Michaeli et al., 2017). By increasing AP-1/NF-AT1 axis activity, Tregs aid HCC in suppressing the immune system (Jiang et al., 2017). Through downregulating the synthesis and secretion of components like granzyme, perforin, TNF-α and IFN-γ, Tregs influence CD8$^+$ T-cell production and cytotoxicity (Fu et al., 2007; Hoechst et al., 2008; Huang et al., 2012). Compared with the low-risk group, our study showed that the expression of Tregs, macrophages and neutrophils in high-risk group was increased. This indicated that the immune function of the high-risk group may be suppressed, which was consistent with the results of immune function analysis. And there were relatively few CD8$^+$ T-cell in the high-risk group. According to a research, immunotherapy is ineffective against tumors lacking CD8$^+$ T-cell infiltration and they have a poorer prognosis (Gajewski, 2015). Those in low-risk group showed greater levels of immune infiltration, higher expression of immune checkpoint genes, and higher IPS scores when compared to patients in high-risk group. Immunotherapy was more likely to be beneficial for patients in low-risk group.

We combined patient prognosis analysis with IIRLs to design a signature which can predict survival rate and therapeutic drugs for the high-risk and the low-risk groups. Though having made some progress, we acknowledged that our research has certain limitations. First, the main data set we collected from TCGA database, lacks an external validation set; Other data sets should be acquired and analyzed to further validate the signature. Second, we did not elucidate the mechanism and function of IIRLs, which deserve further study in the future. Third, no clinical data were found to support the clinical feasibility of treatment drugs in two groups.

Conclusion

We created a signature of immune infiltrationrelated lncRNAs that may be utilized as a novel biomarker to predict HCC development. This signature contributes to a deeper understanding of the correlation between immune infiltration and tumor progression. It is expected to be further utilized in future clinical practice.

Data availability statement

The original contributions presented in the study are included in the article/Supplementary Material, further inquiries can be directed to the corresponding author.

Ethics statement

Our study is based on open-source databases (TCGA and TCIA) with ethical approval of the patients involved.

Author contributions

GL and CW contributed to the conception and design of the study. SX extracted the data and GL analyzed the data. SY and LZ drafted the manuscript. SX contributed to a critical revision of the manuscript. HW completed model guidance, critical review, and funding support. All authors have read and approved the final version of the manuscript.

Funding

Acknowledgments

Conflict of interest

The authors declare that the research was conducted in the absence of any commercial or financial relationships that could be construed as a potential conflict of interest.

Publisher's note

All claims expressed in this article are solely those of the authors and do not necessarily represent those of their affiliated organizations, or those of the publisher, the editors and the reviewers. Any product that may be evaluated in this article, or claim that may be made by its manufacturer, is not guaranteed or endorsed by the publisher.

Supplementary material

The Supplementary Material for this article can be found online at: https://www.frontiersin.org/articles/10.3389/fgene. 2022.1021600/full#supplementary-material

References

Bray, F., Ferlay, J., Soerjomataram, I., Siegel, R. L., Torre, L. A., and Jemal, A. (2018). Global cancer statistics 2018: GLOBOCAN estimates of incidence and mortality worldwide for 36 cancers in 185 countries. *Ca. Cancer J. Clin.* 68 (6), 394–424. doi:10.3322/caac.21492

Chen, H., Liu, Y., Liu, P., Dai, Q., and Wang, P. (2021). LINC01094 promotes the invasion of ovarian cancer cells and regulates the Wnt/β-catenin signaling pathway by targeting miR-532-3p. *Exp. Ther. Med.* 22 (5), 1228. doi:10.3892/etm.2021.10662

Chen, Q., Hu, L., Huang, D., Chen, K., Qiu, X., and Qiu, B. (2020). Six-lncRNA immune prognostic signature for cervical cancer. *Front. Genet.* 11, 533628. doi:10.3389/fgene.2020.533628

Cherkassky, L., Hou, Z., Amador-Molina, A., and Adusumilli, P. S. (2022). Regional CAR T cell therapy: An ignition key for systemic immunity in solid tumors. *Cancer Cell* 40 (6), 569–574. doi:10.1016/j.ccell.2022.04.006

Chidambaranathan-Reghupaty, S., Fisher, P. B., and Sarkar, D. (2021). Hepatocellular carcinoma (HCC): Epidemiology, etiology and molecular classification. *Adv. Cancer Res.* 149, 1–61. doi:10.1016/bs.acr.2020.10.001

Denaro, N., Merlano, M. C., and Lo Nigro, C. (2019). Long noncoding RNAs as regulators of cancer immunity. *Mol. Oncol.* 13 (1), 61–73. doi:10.1002/1878-0261.12413

Dong, X., Fu, X., Yu, M., and Li, Z. (2020). Long intergenic non-protein coding RNA 1094 promotes initiation and progression of glioblastoma by promoting microRNA-577-regulated stabilization of brain-derived neurotrophic factor. *Cancer Manag. Res.* 12, 5619–5631. doi:10.2147/CMAR.S256147

El Khodiry, A., Afify, M., and El Tayebi, H. M. (2018). Behind the curtain of non-coding RNAs; long non-coding RNAs regulating hepatocarcinogenesis. *World J. Gastroenterol.* 24 (5), 549–572. doi:10.3748/wjg.v24.i5.549

European Association for the Study of the Liver (2018). European association for the study of the LiverEASL clinical practice guidelines: Management of hepatocellular carcinoma. *J. Hepatol.* 69 (1), 182–236. doi:10.1016/j.jhep.2018. 03.019

Fridman, W. H., Pages, F., Sautes-Fridman, C., and Galon, J. (2012). The immune contexture in human tumours: Impact on clinical outcome. *Nat. Rev. Cancer* 12 (4), 298–306. doi:10.1038/nrc3245

Friedman, J., Hastie, T., and Tibshirani, R. (2010). Regularization paths for generalized linear models via coordinate descent. *J. Stat. Softw.* 33 (1), 1–22. doi:10. 18637/jss.v033.i01

Fu, J., Xu, D., Liu, Z., Shi, M., Zhao, P., Fu, B., et al. (2007). Increased regulatory T cells correlate with CD8 T-cell impairment and poor survival in hepatocellular carcinoma patients. *Gastroenterology* 132 (7), 2328–2339. doi:10.1053/j.gastro.2007. 03.102

Fu, Y., Liu, S., Zeng, S., and Shen, H. (2019). From bench to bed: The tumor immune microenvironment and current immunotherapeutic strategies for hepatocellular carcinoma. *J. Exp. Clin. Cancer Res.* 38 (1), 396. doi:10.1186/s13046-019-1396-4

Gabrilovich, D. I., and Nagaraj, S. (2009). Myeloid-derived suppressor cells as regulators of the immune system. *Nat. Rev. Immunol.* 9 (3), 162–174. doi:10.1038/nri2506

Gajewski, T. F. (2015). The next hurdle in cancer immunotherapy: Overcoming the non-T-cell-inflamed tumor microenvironment. *Semin. Oncol.* 42 (4), 663–671. doi:10.1053/j.seminoncol.2015.05.011

Galon, J., and Bruni, D. (2019). Approaches to treat immune hot, altered and cold tumours with combination immunotherapies. *Nat. Rev. Drug Discov.* 18 (3), 197–218. doi:10.1038/s41573-018-0007-y

Geeleher, P., Cox, N., and Huang, R. S. (2014). pRRophetic: an R package for prediction of clinical chemotherapeutic response from tumor gene expression levels. *PLoS One* 9 (9), e107468. doi:10.1371/journal.pone.0107468

Geeleher, P., Cox, N. J., and Huang, R. S. (2014). Clinical drug response can be predicted using baseline gene expression levels and *in vitro* drug sensitivity in cell lines. *Genome Biol.* 15 (3), R47. doi:10.1186/gb-2014-15-3-r47

Hanzelmann, S., Castelo, R., and Guinney, J. (2013). Gsva: Gene set variation analysis for microarray and RNA-seq data. *BMC Bioinforma.* 14, 7. doi:10.1186/1471-2105-14-7

Hoechst, B., Ormandy, L. A., Ballmaier, M., Lehner, F., Kruger, C., Manns, M. P., et al. (2008). A new population of myeloid-derived suppressor cells in hepatocellular carcinoma patients induces CD4(+)CD25(+)Foxp3(+) T cells. *Gastroenterology* 135 (1), 234–243. doi:10.1053/j.gastro.2008.03.020

Huang, Y., Wang, F. M., Wang, T., Wang, Y. J., Zhu, Z. Y., Gao, Y. T., et al. (2012). Tumor-infiltrating FoxP3+ Tregs and CD8+ T cells affect the prognosis of hepatocellular carcinoma patients. *Digestion* 86 (4), 329–337. doi:10.1159/000342801

Jemal, A., Ward, E. M., Johnson, C. J., Cronin, K. A., Ma, J., Ryerson, B., et al. (2017). Annual report to the nation on the status of cancer, 1975-2014, featuring survival. *J. Natl. Cancer Inst.* 109 (9), djx030. doi:10.1093/jnci/djx030

Jiang, R., Tang, J., Chen, Y., Deng, L., Ji, J., Xie, Y., et al. (2017). The long noncoding RNA lnc-EGFR stimulates T-regulatory cells differentiation thus promoting hepatocellular carcinoma immune evasion. *Nat. Commun.* 8, 15129. doi:10.1038/ncomms15129

Jiang, Y., Li, W., Yan, Y., Yao, X., Gu, W., and Zhang, H. (2020). LINC01094 triggers radio-resistance in clear cell renal cell carcinoma via miR-577/CHEK2/FOXM1 axis. *Cancer Cell Int.* 20, 274. doi:10.1186/s12935-020-01306-8

Kim, S., Kim, A., Shin, J. Y., and Seo, J. S. (2020). The tumor immune microenvironmental analysis of 2, 033 transcriptomes across 7 cancer types. *Sci. Rep.* 10 (1), 9536. doi:10.1038/s41598-020-66449-0

Kulik, L., and El-Serag, H. B. (2019). Epidemiology and management of hepatocellular carcinoma. *Gastroenterology* 156 (2), 477–491. doi:10.1053/j. gastro.2018.08.065

Langfelder, P., and Horvath, S. (2008). Wgcna: an R package for weighted correlation network analysis. *BMC Bioinforma.* 9, 559. doi:10.1186/1471-2105-9-559

Lawal, G., Xiao, Y., Rahnemai-Azar, A. A., Tsilimigras, D. I., Kuang, M., Bakopoulos, A., et al. (2021). The immunology of hepatocellular carcinoma. *Vaccines (Basel)* 9 (10), 1184. doi:10.3390/vaccines9101184

Li, B., Severson, E., Pignon, J. C., Zhao, H., Li, T., Novak, J., et al. (2016). Comprehensive analyses of tumor immunity: Implications for cancer immunotherapy. *Genome Biol.* 17 (1), 174. doi:10.1186/s13059-016-1028-7

Li, T., Fan, J., Wang, B., Traugh, N., Chen, Q., Liu, J. S., et al. (2017). Timer: A web server for comprehensive analysis of tumor-infiltrating immune cells. *Cancer Res.* 77 (21), e108–e110. doi:10.1158/0008-5472.CAN-17-0307

Li, T., Fu, J., Zeng, Z., Cohen, D., Li, J., Chen, Q., et al. (2020). TIMER2.0 for analysis of tumor-infiltrating immune cells. *Nucleic Acids Res.* 48 (W1), W509–W14. doi:10.1093/nar/gkaa407

Li, X. X., and Yu, Q. (2020). Linc01094 accelerates the growth and metastatic-related traits of glioblastoma by sponging miR-126-5p. *Onco. Targets. Ther.* 13, 9917–9928. doi:10.2147/OTT.S263091

Liu, L., Xu, Q., Xiong, Y., Deng, H., and Zhou, J. (2022). LncRNA LINC01094 contributes to glioma progression by modulating miR-224-5p/CHSY1 axis. *Hum. Cell* 35 (1), 214–225. doi:10.1007/s13577-021-00637-6

Llovet, J. M., Bru, C., and Bruix, J. (1999). Prognosis of hepatocellular carcinoma: The BCLC staging classification. *Semin. Liver Dis.* 19 (3), 329–338. doi:10.1055/s-2007-1007122

Llovet, J. M., Castet, F., Heikenwalder, M., Maini, M. K., Mazzaferro, V., Pinato, D. J., et al. (2022). Immunotherapies for hepatocellular carcinoma. *Nat. Rev. Clin. Oncol.* 19 (3), 151–172. doi:10.1038/s41571-021-00573-2

Llovet, J. M., Kelley, R. K., Villanueva, A., Singal, A. G., Pikarsky, E., Roayaie, S., et al. (2021). Hepatocellular carcinoma. *Nat. Rev. Dis. Prim.* 7 (1), 6. doi:10.1038/s41572-020-00240-3

Llovet, J. M., Villanueva, A., Marrero, J. A., Schwartz, M., Meyer, T., Galle, P. R., et al. (2021). Trial design and endpoints in hepatocellular carcinoma: AASLD consensus conference. *Hepatology* 73, 158–191. doi:10.1002/hep.31327

Luo, C., Lin, K., Hu, C., Zhu, X., Zhu, J., and Zhu, Z. (2021). LINC01094 promotes pancreatic cancer progression by sponging miR-577 to regulate LIN28B expression and the PI3K/AKT pathway. *Mol. Ther. Nucleic Acids* 26, 523–535. doi:10.1016/j.omtn.2021.08.024

Ma, W., Zhao, F., Yu, X., Guan, S., Suo, H., Tao, Z., et al. (2020). Immune-related lncRNAs as predictors of survival in breast cancer: A prognostic signature. *J. Transl. Med.* 18 (1), 442. doi:10.1186/s12967-020-02522-6

Masucci, M. T., Minopoli, M., and Carriero, M. V. (2019). Tumor associated neutrophils. Their role in tumorigenesis, metastasis, prognosis and therapy. *Front. Oncol.* 9, 1146. doi:10.3389/fonc.2019.01146

Mathias, C., Muzzi, J. C. D., Antunes, B. B., Gradia, D. F., Castro, M. A. A., and Carvalho de Oliveira, J. (2021). Unraveling immune-related lncRNAs in breast cancer molecular subtypes. *Front. Oncol.* 11, 692170. doi:10.3389/fonc.2021.692170

Michaeli, J., Shaul, M. E., Mishalian, I., Hovav, A. H., Levy, L., Zolotriov, L., et al. (2017). Tumor-associated neutrophils induce apoptosis of non-activated CD8 T-cells in a TNFα and NO-dependent mechanism, promoting a tumor-supportive environment. *Oncoimmunology* 6 (11), e1356965. doi:10.1080/2162402X.2017.1356965

Newman, A. M., Liu, C. L., Green, M. R., Gentles, A. J., Feng, W., Xu, Y., et al. (2015). Robust enumeration of cell subsets from tissue expression profiles. *Nat. Methods* 12 (5), 453–457. doi:10.1038/nmeth.3337

Nicolas-Avila, J. A., Adrover, J. M., and Hidalgo, A. (2017). Neutrophils in homeostasis, immunity, and cancer. *Immunity* 46 (1), 15–28. doi:10.1016/j.immuni.2016.12.012

Pinero, F., Dirchwolf, M., and Pessoa, M. G. (2020). Biomarkers in hepatocellular carcinoma: Diagnosis, prognosis and treatment response assessment. *Cells* 9 (6), 1370. doi:10.3390/cells9061370

Qian, B. Z., and Pollard, J. W. (2010). Macrophage diversity enhances tumor progression and metastasis. *Cell* 141 (1), 39–51. doi:10.1016/j.cell.2010.03.014

Ritchie, M. E., Phipson, B., Wu, D., Hu, Y., Law, C. W., Shi, W., et al. (2015). Limma powers differential expression analyses for RNA-sequencing and microarray studies. *Nucleic Acids Res.* 43 (7), e47. doi:10.1093/nar/gkv007

Wang, D., Garcia-Bassets, I., Benner, C., Li, W., Su, X., Zhou, Y., et al. (2011). Reprogramming transcription by distinct classes of enhancers functionally defined by eRNA. *Nature* 474 (7351), 390–394. doi:10.1038/nature10006

Wang, K. C., and Chang, H. Y. (2011). Molecular mechanisms of long noncoding RNAs. *Mol. Cell* 43 (6), 904–914. doi:10.1016/j.molcel.2011.08.018

Wang, Z., Liu, Y., Zhang, J., Zhao, R., Zhou, X., and Wang, H. (2021). An immune-related long noncoding RNA signature as a prognostic biomarker for human endometrial cancer. *J. Oncol.* 2021, 9972454. doi:10.1155/2021/9972454

Wu, M., Fu, P., Qu, L., Liu, J., and Lin, A. (2020). Long noncoding RNAs, new critical regulators in cancer immunity. *Front. Oncol.* 10, 550987. doi:10.3389/fonc.2020.550987

Wu, T., Hu, E., Xu, S., Chen, M., Guo, P., Dai, Z., et al. (2021). clusterProfiler 4.0: A universal enrichment tool for interpreting omics data. *Innovation.* 2 (3), 100141. doi:10.1016/j.xinn.2021.100141

Wu, X., Kong, C., and Wu, Y. (2021). Long intergenic non-protein coding RNA 1094 (LINC01094) promotes the progression of breast cancer (BC) by regulating the microRNA-340-5p (miR-340-5p)/E2F transcription factor 3 (E2F3) axis. *Bioengineered* 12 (1), 9046–9057. doi:10.1080/21655979.2021.1993715

Xie, C., Li, S. Y., Fang, J. H., Zhu, Y., and Yang, J. E. (2021). Functional long non-coding RNAs in hepatocellular carcinoma. *Cancer Lett.* 500, 281–291. doi:10.1016/j.canlet.2020.10.042

Xu, H., Wang, X., Wu, J., Ji, H., Chen, Z., Guo, H., et al. (2020). Long non-coding RNA LINC01094 promotes the development of clear cell renal cell carcinoma by upregulating SLC2A3 via MicroRNA-184. *Front. Genet.* 11, 562967. doi:10.3389/fgene.2020.562967

Xu, J., Zhang, P., Sun, H., and Liu, Y. (2020). LINC01094/miR-577 axis regulates the progression of ovarian cancer. *J. Ovarian Res.* 13 (1), 122. doi:10.1186/s13048-020-00721-9

Yan, K., Fu, Y., Zhu, N., Wang, Z., Hong, J. L., Li, Y., et al. (2019). Repression of lncRNA NEAT1 enhances the antitumor activity of CD8(+)T cells against hepatocellular carcinoma via regulating miR-155/Tim-3. *Int. J. Biochem. Cell Biol.* 110, 1–8. doi:10.1016/j.biocel.2019.01.019

Yao, R. R., Li, J. H., Zhang, R., Chen, R. X., and Wang, Y. H. (2018). M2-polarized tumor-associated macrophages facilitated migration and epithelial-mesenchymal transition of HCC cells via the TLR4/STAT3 signaling pathway. *World J. Surg. Oncol.* 16 (1), 9. doi:10.1186/s12957-018-1312-y

Yau, T., Kang, Y. K., Kim, T. Y., El-Khoueiry, A. B., Santoro, A., Sangro, B., et al. (2020). Efficacy and safety of nivolumab plus ipilimumab in patients with advanced hepatocellular carcinoma previously treated with sorafenib: The CheckMate 040 randomized clinical trial. *JAMA Oncol.* 6 (11), e204564. doi:10.1001/jamaoncol.2020.4564

Yoshihara, K., Shahmoradgoli, M., Martinez, E., Vegesna, R., Kim, H., Torres-Garcia, W., et al. (2013). Inferring tumour purity and stromal and immune cell admixture from expression data. *Nat. Commun.* 4, 2612. doi:10.1038/ncomms3612

Yu, G., Wang, L. G., Han, Y., and He, Q. Y. (2012). clusterProfiler: an R package for comparing biological themes among gene clusters. *OMICS* 16 (5), 284–287. doi:10.1089/omi.2011.0118

Yu, W. D., Wang, H., He, Q. F., Xu, Y., and Wang, X. C. (2018). Long noncoding RNAs in cancer-immunity cycle. *J. Cell. Physiol.* 233 (9), 6518–6523. doi:10.1002/jcp.26568

Zhang, J., Zhang, Q., Lou, Y., Fu, Q., Chen, Q., Wei, T., et al. (2018). Hypoxia-inducible factor-1α/interleukin-1β signaling enhances hepatoma epithelial-mesenchymal transition through macrophages in a hypoxic-inflammatory microenvironment. *Hepatology* 67 (5), 1872–1889. doi:10.1002/hep.29681

Zhu, B., Liu, W., Liu, H., Xu, Q., and Xu, W. (2020). LINC01094 down-regulates miR-330-3p and enhances the expression of MSI1 to promote the progression of glioma. *Cancer Manag. Res.* 12, 6511–6521. doi:10.2147/CMAR.S254630